Corrections of order $\alpha^2(Z\alpha)^5$ to the hyperfine splitting and the Lamb shift

Michael I. Eides*
Petersburg Nuclear Physics Institute, Gatchina, St. Petersburg 188350, Russia

Valery A. Shelyuto
D. I. Mendeleev Institute of Metrology, St. Petersburg 198005, Russia
(Received 1 February 1995)

Corrections to the hyperfine splitting and the Lamb shift of order $\alpha^2(Z\alpha)^5$ induced by diagrams with radiative photon insertions in the electron line are calculated in the Fried-Yennie gauge. These contributions are as large as $-7.724(1)\alpha^2(Z\alpha)^5/(\pi n^3)(m_r/m)^3 m$ and $-0.6726(4)\ \alpha^2(Z\alpha)/(\pi n^3)E_F$ for the Lamb shift and the hyperfine splitting, respectively. Here m is the electron mass, m_r is the reduced mass, n is the main quantum number, and E_F is the Fermi energy of the hyperfine splitting. Phenomenological implications of these results are discussed with special emphasis on the accuracy of the theoretical predictions for the Lamb shift and the experimental determination of the Rydberg constant. A precise value of the Rydberg constant is obtained on the basis of the improved theory and experimental data.

PACS number(s): 12.20.Ds, 31.30.Jv, 36.10.Dr, 06.20.Jr

Steady and rapid progress in spectroscopic measurements in recent years has led to a dramatic increase in accuracy of the measurements of the Rydberg constant [1,2], the ground state $1S$ Lamb shift in hydrogen and deuterium [2–4], the classic $2S_{1/2}$-$2P_{1/2}$ Lamb shift in hydrogen [5–8], and the muonium hyperfine splitting in the ground state [9,10] (see Table I). These spectacular experimental achievements constitute a serious challenge to the theory and intensive theoretical efforts are necessary to match this experimental accuracy.

Theoretical work on the high-order corrections to the hyperfine splitting (hfs) and the Lamb shift concentrated recently on the calculation of nonrecoil contributions of order $\alpha^2(Z\alpha)^5$. Their magnitude may run up to several kilohertz for the hfs in the ground state of muonium, to several tens of kilohertz for the $n = 2$ Lamb shift in hydrogen, and may be as large as hundreds of kilohertz for the ground-state Lamb shift in hydrogen. Contributions of such orders of magnitude are clearly crucial for a comparison of the current and pending experimental results with the theory.

As shown in [11] for the hyperfine splitting and in [12] for the Lamb shift there are six gauge invariant sets of diagrams (see Fig. 1), that produce corrections of order $\alpha^2(Z\alpha)^5$. All these diagrams may be obtained from the skeleton diagram, which contains two external photons attached to the electron line, with the help of different radiative insertions. All contributions induced by the diagrams in Figs. 1(a)–1(e), containing closed electron loops, were obtained recently in papers [11,13–15] for the case of the hyperfine splitting and in papers [12,16–19] for the case of the Lamb shift. These theoretical results are now firmly established since all these corrections were calculated independently by two different groups and the results of these calculations are in excellent agreement.

We report in this paper on the results of our calculation of the contributions of order $\alpha^2(Z\alpha)^5$ to the hfs and the Lamb shift induced by the gauge invariant set of diagrams in Fig. 1(f). This set includes 19 topologically different diagrams [20] presented in Fig. 2. The simplest way to describe these graphs is to realize that they are obtained from the three graphs for the two-loop electron self-energy by insertion of two external photons in all possible ways. Indeed, graphs 2(a)–2(c) are obtained from the two-loop reducible electron self-energy diagram, graphs 2(d)–2(k) are the result of all possible insertions of two external photons in the rainbow self-energy di-

TABLE I. Experimental results.

Interval	ΔE (kHz)
hydrogen, $1S_{1/2}$ [3]	8172860(60)
hydrogen, $1S_{1/2}$ [2]	8172815(70)
hydrogen, $1S_{1/2}$ [4]	8172844(55)
hydrogen, $2S_{1/2}$-$2P_{1/2}$ [5]	1057845(9)
hydrogen, $2S_{1/2}$-$2P_{1/2}$ [6,7]	1057857.6(2.1)
hydrogen, $2S_{1/2}$-$2P_{1/2}$ [8]	1057839(12)
muonium, hfs [9]	4463302.88(16)

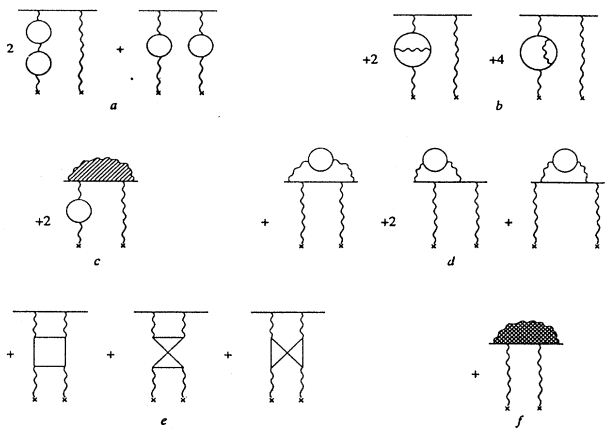

FIG. 1. Six gauge invariant sets of graphs producing corrections of order $\alpha^2(Z\alpha)^5$.

 ©1995 The American Physical Society

agram, and diagrams 2(l)–2(s) are connected with the overlapping two-loop self-energy graph. We have calculated the contributions induced by the diagrams in Figs. 2(a)–2(h) and 2(l) earlier [20,21]. Results of the calculation of the contributions produced by the remaining diagrams in Fig. 2 are presented below.

While this work was in progress two other papers were published where the contributions of the diagrams in Fig. 2 to the hfs [15] and the Lamb shift [22] were calculated. Our results confirm the results of the previous authors, but are about two orders of magnitude more precise (see comments below).

Let us start with a brief description of the main features of our approach to the calculations. As shown in [23] for the hfs and in [12] for the Lamb shift, contributions to the energy splittings are given by the matrix elements of the diagrams in Fig. 2 calculated between free electron spinors with all external electron lines on the mass shell, projected on the respective spin states, and multiplied by the square at the origin of the Schrödinger-Coulomb wave function.

The actual calculation of the matrix elements is impeded by the ultraviolet and infrared divergences. Infrared problems are as usual more difficult to deal with than the ultraviolet ones. It is easy to realize that in the standard Feynman gauge, all diagrams in Fig. 2 are infrared divergent and one has to introduce the radiative photon mass to regularize this divergence. Certainly, the final result for the sum of all contributions induced by the diagrams in Fig. 2 is infrared finite and should admit a smooth limit for the vanishing photon mass. However, numerical recipes used in the calculations of the contributions to the energy shifts make it impossible to check analytically the independence of the results from the photon mass and one has to rely on the extrapolation in the infrared photon mass. Of course, such an approach is still feasible, but we have preferred to use the gauge invariance of the sum of diagrams in Fig. 2 and perform all calculations in the Fried-Yennie (FY) gauge [24] for the radiative photons. All diagrams are infrared finite in this remarkable gauge and one may perform the on-mass-shell renormalization without the introduction of the infrared photon mass (see, e.g., [23]), thus avoiding the problem of extrapolation to the vanishing photon mass. Of course, infrared finiteness in the FY gauge is not given for free and one has to pay special attention to the infrared behavior of the integrand functions and perform cancellation of spurious infrared divergences with the help of integration by parts over the Feynman parameters prior to momentum integration.

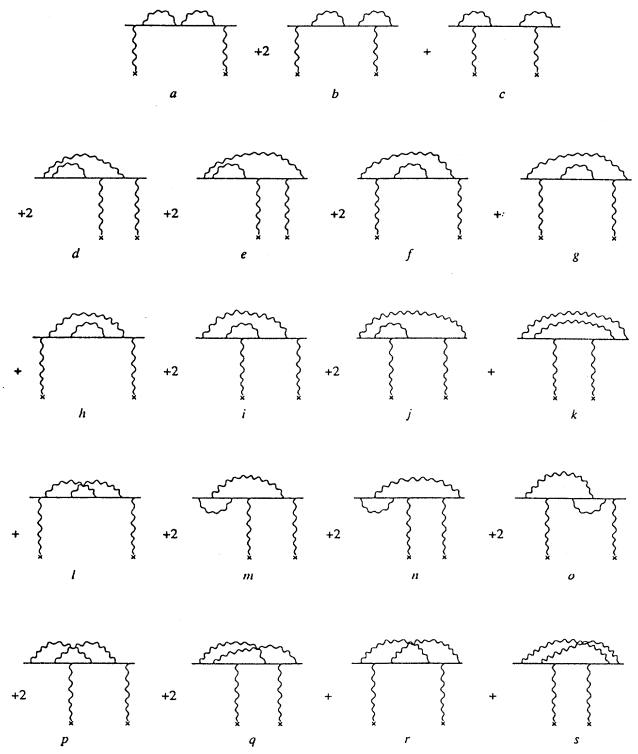

FIG. 2. Nineteen topologically different diagrams with two radiative photon insertions in the electron line.

The calculation of the contributions to the energy splittings starts with writing down the universal infrared diverging skeleton integrals corresponding to the electron line with two external photons. Each contribution of order $\alpha^2(Z\alpha)^5$ arises from radiative insertions in the skeleton graph. Corrections to the hyperfine splitting and the Lamb shift, produced by the diagrams in Figs. 1 and 2, are given by the expressions (see, e.g., [23,12])

$$\Delta E_{\rm hfs} = 8\,\frac{Z\alpha}{\pi n^3}\left(\frac{\alpha}{\pi}\right)^2 E_F \int_0^\infty \frac{dk}{k^2}\, L_{\rm hfs}(k) \qquad (1)$$

and

$$\Delta E_L = -16\,\frac{(Z\alpha)^5}{\pi n^3}\left(\frac{\alpha}{\pi}\right)^2 \left(\frac{m_r}{m}\right)^3 m \int_0^\infty \frac{dk}{k^4}\, L_L(k)\,, \qquad (2)$$

where k is the magnitude of the three-dimensional momentum of the external photons measured in the electron mass units, $m_r = m/(1+m/M)$ is the reduced mass of the electron-muon (or electron-proton) system, and E_F is the Fermi energy of the hyperfine splitting. The functions $L(k)$ are connected with the numerator structure and the spin projection of each particular graph and describe radiative corrections to the skeleton diagram. They are normalized on the skeleton numerator contributions.

It should be mentioned that some of the diagrams under consideration also contain contributions of the previous order in $Z\alpha$. The physical nature of these contributions is especially transparent in the case of the hfs. They correspond to anomalous magnetic moment, their true order in $Z\alpha$ is lower than their apparent order, and they should be subtracted from the electron factor prior to the calculation of the contributions to the hfs. An analogous situation holds also in the case of the Lamb shift. The only difference is that this time not only the Pauli form factor but also the slope of the Dirac form factor of the electron is capable of producing a lower-order contribution to the splitting of the energy levels (see,

e.g., [12,16,17]). Technically, cases of lower-order contributions both to the hfs and to the Lamb shift are quite similar. Lower-order terms are produced by the constant terms in the low-frequency asymptotic expansion of the electron factor in the case of the hyperfine splitting and by the terms proportional to the exchanged momentum squared in the low-frequency asymptotic expansion of the electron factor in the case of the Lamb shift.

These lower-order contributions are connected with integration over external photon momenta of characteristic atomic order $mZ\alpha$ and the approximation based on the skeleton integrals in Eqs. (1) and (2) is inadequate for their calculation. In the skeleton integral approach these previous-order contributions emerge as the infrared divergences induced by the low-frequency terms in the electron factors. We subtract leading low-frequency terms in the low-frequency asymptotic expansions of the electron factors, when necessary, and thus get rid of the previous-order contributions.

The results of our calculations of the contributions to the hfs and the Lamb shift produced by different diagrams in the FY gauge are presented in Table II.[1] For the total correction of order $\alpha^2(Z\alpha)^5$ to the hfs and the Lamb shift produced by all diagrams in Fig. 2 we obtain

$$\Delta E^{(1f)}_{\rm hfs} = -0.\ 6726\ (4)\ \frac{\alpha^2(Z\alpha)}{\pi n^3}\ E_F \qquad (3)$$

and

$$\Delta E^{(1f)}_{L} = -7.\ 724\ (1)\ \frac{\alpha^2(Z\alpha)^5}{\pi n^3}\ \left(\frac{m_r}{m}\right)^3\ m. \qquad (4)$$

As already mentioned above, the contributions of the diagrams in Fig. 2 to the hfs and to the Lamb shift were originally calculated in [15] and [22], respectively. The authors of these works used a completely different approach to calculations; in particular, they worked in the Feynman gauge and hence all contributions of individual diagrams in these works are infrared divergent. These divergences are regulated with the help of an auxiliary infrared photon mass. The numbers cited in [15,22] emerge as a finite sum of large spurious contributions produced by individual diagrams. Despite the great differences in the approaches used in the present work and in [15,22], numerical factors in Eqs. (3) and (4) are compatible with $-0.63(4)$ in [15] and with $-7.61(16)$ in [22], respectively. Our numbers are about two orders of magnitude more precise and further improvement of accuracy may be achieved. The reason for this increased accuracy is the use of the FY gauge, where one can avoid spurious infrared divergences. The price we had paid for this advantage is the more tiresome analytic work needed to cancel all would-be infrared divergences before integration.

Numerically the correction to muonium hfs in the ground state produced by the diagrams in Fig. 2 is equal to

TABLE II. Corrections to the hfs and the Lamb shift.

Diagram	hfs $\left(\frac{\alpha^2(Z\alpha)}{\pi n^3}E_F\right)$	Lamb shift $\left[\frac{\alpha^2(Z\alpha)^5}{\pi n^3}\left(\frac{m_r}{m}\right)^3 m\right]$
a	9/4	0
b	−6.65997(1)	2.9551(1)
c	3.93208(1)	−2.2231(1)
d	-3.903368(79)	−5.238023(56)
e	4.566710(24)	5.056278(81)
f	−3.404163(22)	−1.016145(21)
g	2.684706(26)	−0.1460233(52)
h	33/16	153/80
i	0.054645(46)	−5.51683(34)
j	−7.14937(16)	−7.76815(17)
k	1.465834(20)	1.959589(33)
l	−1.983298(95)	1.74815(38)
m	3.16956(16)	1.87540(17)
n	−3.59566(14)	−1.30584(18)
o	1.804775(46)	−12.06751(47)
p	3.50608(16)	6.13776(25)
q	−0.80380(15)	−7.52453(34)
r	1.05298(18)	14.36733(44)
s	0.277203(27)	−0.930268(72)
total	−0.6726(4)	−7.724(1)

$$\Delta E^{(1f)}_{\rm hfs} = -0.3710(2)\ {\rm kHz} \qquad (5)$$

and the total contribution of order $\alpha^2(Z\alpha)E_F$ is given by

$$\Delta E^{(1a-1f)}_{\rm hfs} = 0.\ 4256(2)\ {\rm kHz}. \qquad (6)$$

Taking into account other theoretical contributions to the hfs and especially some small contributions obtained recently (see, e.g., reviews in [15,25]) and using for the calculation the value of the fine structure constant as obtained in [26], one may obtain the theoretical value for the muonium hfs in the ground state

$$\Delta E_{\rm hfs} = 4\,463\,302.55(0.18)(0.18)(1.33)\ {\rm kHz}, \qquad (7)$$

where the first error in parentheses reflects the uncertainty of the fine structure constant itself and the second is induced by the uncertainty of the contribution of order $\alpha(Z\alpha)^2E_F$. The third, and by far the largest contribution to the error in the theoretical value of the hfs, is defined by the experimental error in measuring electron-muon mass ratio m/M.

The agreement between theory and experiment is excellent. We will not dwell on the hfs problem anymore here since the phenomenological situation and the influence of the result in Eq. (3) on the value of the electron-muon mass ratio and the fine structure constant was discussed in great detail recently [15,25].

The case of the Lamb shift deserves more comments. Numerically the corrections to the $1S$ and $2S$ Lamb shifts produced by the diagrams in Fig. 2 are equal to

[1] A detailed account of our calculations will be presented in a separate publication.

$$\Delta E_L^{(1f)}(1S) = -334.21(4)\ \text{kHz}, \quad (8)$$

$$\Delta E_L^{(1f)}(2S) = -41.776(5)\ \text{kHz},$$

while respective total contributions of order $\alpha^2(Z\alpha)^5 m$ are given by

$$\Delta E_L^{(1a-1f)}(1S) = -296.90(4)\ \text{kHz}, \quad (9)$$

$$\Delta E_L^{(1a-1f)}(2S) = -37.112(5)\ \text{kHz}.$$

Let us discuss the sign and the scale of the correction in Eq. (8). The sign may be determined by considering the electron factor, as defined in Eq. (2). The low-frequency asymptotic behavior of the electron factor is described by the expression (see, e.g., [17])

$$L(k) \approx [-2F_1'(0) - \tfrac{1}{2}F_2(0)]\, k^2 = -0.704\,622\,5k^2, \quad (10)$$

where $F_1(k^2)$ and $F_2(k^2)$ are the two-loop contributions to the ordinary Dirac and Pauli form factors of the electron [the contribution of the graphs with vacuum polarization insertions in the photon line is omitted in Eq. (10)], respectively. We use in Eq. (10) the well-known values for the slope of the Dirac form factor and of the Pauli form factor at zero [27,28]. As explained above, one has to subtract from the electron factor this leading low-frequency term, which produces the contribution to the Lamb shift of previous order in $Z\alpha$.

It is well known from the general principles that the unsubtracted electron factor has at most logarithmic behavior at infinity. Hence the high momentum behavior of the subtracted electron factor is completely defined by the subtraction term in Eq. (10). Then it is clear from Eq. (2), where the subtracted electron factor plays the role of the integrand, that the contribution to the Lamb shift induced by the graphs in Fig. 2 has the negative sign. One may even make an estimate of this contribution from the known asymptotic behavior of the integrand, but we choose a less technical path in the discussion of the magnitude of this contribution.

It may seem at first sight that the magnitude of the corrections induced by the diagrams in Fig. 1(f) as presented in Eq. (8) are too large. We would like to emphasize that, quite oppositely, this correction has exactly the scale one had to envisage before calculations. Let us discuss this point in slightly more detail. It is helpful to recollect that the main contribution to the Lamb shift is a radiative correction itself and so it is misleading to normalize all contributions to the Lamb shift with the help of this leading-order contribution. In this respect the case of the Lamb shift differs drastically from the case of the hfs, where the leading Fermi contribution is not the radiative correction but the classic effect of the interaction of two magnetic moments and sets the natural scale for all radiative corrections. The main contribution to the Lamb shift has the form $4m(Z\alpha)^4/n^3$ times the slope of the Dirac form factor, where the slope is, roughly speaking, $(\alpha/\pi)(1/3)\ln(Z\alpha)^{-2}$. The skeleton factor that sets the scale for the different contributions to the Lamb shift is $4m(Z\alpha)^4/n^3$ and to make an estimate of any correction to the Lamb shift one has to extract this skeleton factor. All other entries in the leading-order contribution to the Lamb shift are produced by the radiative correction, and it is necessary to take into account that the number that should be of order one, as predicted by the common wisdom for radiative corrections, is the factor $1/3$ before the logarithm, which remains after extraction of the factor α/π, characteristic for the one-loop radiative corrections. The other subtlety to be taken into account in estimating the orders of magnitude of different corrections is that, unlike the case of radiative corrections to the scattering amplitudes, in the bound state problem not every factor α is accompanied by an extra factor π in the denominator. This is a well known feature of the Coulomb problem.

Let us consider as an exercise in the art of making educated estimates the correction of order $\alpha(Z\alpha)^5 m$ calculated analytically a long time ago [29,30]. According to the considerations above, the scale of this correction should be set by the factor $4\alpha(Z\alpha)^5/n^3 m$ and the only problem of the theory is to calculate the number of order one before this factor. The analytic calculation [29,30] produces this factor in the form $1 + \frac{11}{128} - \frac{1}{2}\ln 2 \approx 0.739$, in excellent agreement with our qualitative considerations. Now it is easy to realize that the natural scale for the correction of order $\alpha^2(Z\alpha)^5$ is set by the factor $4\alpha^2(Z\alpha)^5/(\pi n^3)m$. The coefficient before this factor, obtained above and in [22], is about -1.9 and there is nothing unusual in its magnitude for a numerical factor corresponding to a radiative correction.

Consider now the current status of the Lamb shift theory. Theoretical predictions presented below are obtained with the help of the expressions for the Lamb shift contributions as collected in the reviews [31,32], amended, besides corrections obtained above and in [22], with some other recent results presented in Table III. Note that the correction of order $\alpha^2(Z\alpha)^6$ in this table is again of reasonable magnitude since its scale is set by the factor $4\alpha^2(Z\alpha)^6/(\pi^2 n^3)m$, as one may easily check with

TABLE III. Contributions to the Lamb shift.

Level	ΔE
$nS_{1/2}$[a]	$-\frac{8}{27}\frac{\alpha^2(Z\alpha)^6}{\pi^2 n^3}\ln^3[Z\alpha]^{-2}(\frac{m_r}{m})^3 m$
$nS_{1/2}$[b]	$(4\ln 2 - \frac{7}{2})\frac{(Z\alpha)^6}{n^3}\frac{m}{M}m$
$nS_{1/2}$[c]	$(\frac{2\pi^2}{9} - \frac{70}{27})\frac{m}{M}\frac{\alpha(Z\alpha)^5}{\pi^2 n^3}(\frac{m_r}{m})^3 m$
nP_j[d]	$\{[(\frac{217}{480} + \frac{3}{16n} - \frac{14}{15n^2} + \frac{1}{2n^3} - \sigma 1(\frac{7}{192} + \frac{3}{32n} - \frac{1}{6n^2})]\frac{(Z\alpha)^6}{n^3} + \sigma 1\frac{0.328}{3}\frac{\alpha^2(Z\alpha)^4}{\pi^2 n^3}\}\frac{m}{M}m$
$nS_{1/2}$[e]	$-4\left[\frac{1}{15}(\frac{m}{m_\mu})^2 + \sum_{v_i}\frac{4\pi^2}{f_{v_i}^2 m_{v_i}^2} + \frac{2}{3}\frac{1}{1\ \text{GeV}^2}\right]\frac{\alpha(Z\alpha)^4}{\pi n^3}m$

[a]Reference [34].
[b]Reference [40].
[c]Reference [41].
[d]Reference [42].
[e]This work.

the help of the arguments used above in the discussion of the contribution of order $\alpha^2(Z\alpha)^5$. On the background of this factor the numerical factor 2/27 before the cube of the logarithm is quite moderate.

The last line in Table III contains a recoil correction corresponding to the insertions in the Coulomb photon of the muon or hadron vacuum polarization operators.[2] The respective contribution for the muon insertion contains an evident extra electron-muon mass ratio squared suppression factor relative to the leading vacuum polarization contribution. We estimated the hadron contribution approximating the spectral function below 1 GeV according to the vector dominance model and above 1 GeV we simply used the asymptotic quark value for the spectral function.[3]

We use in the calculation of the theoretical values for the Lamb shift values [33] for the self-energy contributions to the coefficient C_{60} for the $1S$ and $2S$ states and [34] to the function $G_{\rm SE}$ for the $2P_{1/2}$ state and [35] for the $4S_{1/2}$ state. We also use values [35] $G_{\rm VP}(1S_{1/2}) = -0.6187$, $G_{\rm VP}(2S_{1/2}) = -0.8089$, $G_{\rm VP}(2P_{1/2}) = -0.0640$, and $G_{\rm VP}(4S_{1/2}) = -0.8066$ for the Uehling part of the vacuum polarization contribution. These numbers are the sum of contributions of order $\alpha(Z\alpha)^6$ and of additional terms of higher order in $Z\alpha$.

From the theoretical point of view the accuracy of the calculations is limited by the magnitude of the yet uncalculated contributions to the Lamb shift. First, there is an unknown correction of order $\alpha^3(Z\alpha)^4$, which is induced by the three-loop slope of the Dirac form factor of the electron and by the three-loop electron vacuum polarization. A natural scale for this correction is set by the factor $4\alpha^3(Z\alpha)^4/(\pi^3 n^3)m$ and we envisage the contributions about 17 kHz for the $1S$ state and 2 kHz for the $2S$ state.

Next come uncalculated corrections of order $\alpha^2(Z\alpha)^6$. A contribution of this order is a polynomial in $\ln(Z\alpha)^{-2}$, starting with the cube of the logarithm. The factor before the cube of the logarithm was calculated in [34] and the contribution of the square of the logarithm terms to the difference $E_L(1S) - 8E_L(2S)$ was obtained in [7]. However, the calculation of respective contributions to the separate energy levels is still missing. In these conditions it is fair to take the square of the logarithm contribution to the interval $E_L(1S) - 8E_L(2S)$ as an estimate of the scale of all yet uncalculated corrections of this order. We thus assume that uncertainties induced by the yet uncalculated contributions of order $\alpha^2(Z\alpha)^6$ constitute 15 kHz and 2 kHz for the $1S$ and $2S$ states, respectively.

The scale of the self-energy correction of order $\alpha(Z\alpha)^7$ is set by the factor $4\alpha(Z\alpha)^7/n^3$. This contribution is a linear polynomial in $\ln(Z\alpha)^{-2}$. We are aware of two recent attempts to make an estimate of this contribution [36,7], but, unfortunately, its final magnitude seems to be still unavailable.[4] Relying on the scale factor above and the estimates in [36,7], we assume that the corrections of order $\alpha(Z\alpha)^7$ are as large as 17 kHz and 2 kHz to the $1S$ and $2S$ states, respectively.

All other theoretical contributions to the Lamb shift are smaller than those just discussed. Hence we assume that the theoretical uncertainty of the expression for the Lamb shift is about 28 kHz for the $1S$ state and about 4 kHz for the $2S$ state.

The other limit on the accuracy of the theoretical calculation of the Lamb shift is set by the accuracy of the measurements of the proton rms charge radius. As is well known, there are two contradictory experimental results for this radius [37,38] and at least one of these experimental results should be in error. The accuracy of the proton rms charge radius claimed by the authors of [37,38] produces an uncertainty of about 32 kHz for the $1S$ state and about 4 kHz for the $2S$ state.

Let us compare theoretical and experimental data for the classic $2S_{1/2}$-$2P_{1/2}$ Lamb shift. The most precise experimental data, as well as the results of our theoretical calculations, are presented in Table IV. Theoretical results for the energy shifts in Table IV contain errors in the parentheses where the first error is determined by the yet uncalculated contributions to the Lamb shift, discussed above, and the second reflects the experimental uncertainty in the measurement of the proton rms charge radius. We have used the experimental result [6] taking into account recent theoretical correction discovered in [7]. Note, however, that this correction does not effect any of our conclusions. There are two immediate conclusions from the data in Table IV. First, as already mentioned in [22], the results from the proton rms radius measurement in [37] should be in error since the respective value of the proton charge radius is clearly inconsistent with all results of the Lamb shift measurements. Second, we have to reject either the result of the most precise measurement of the $2S_{1/2}$-$2P_{1/2}$ splitting or the experimental value of the proton charge radius as measured in [38] since the Lamb shift value in [6] contradicts theoretical value calculated by employing the rms radius in [38] by more than five standard deviations. The results of two other measurements of the classic Lamb shift are compatible with the theory, so we will accept below the value of the proton charge radius as obtained in [38]. Below we will return to the numbers in the three last lines in Table IV.

We do not include theoretical predictions for the deuterium Lamb shift in Table IV since, taking into account current discrepancies in the determination of the deuteron charge radius and solid status of the Lamb shift theory, it seems preferable to use the deuteron Lamb shift data for extracting the value of this charge radius rather than for the comparison of the Lamb shift theory and experiment.

---

[2] S. Karshenboim has also considered these contributions [S. Karshenboim, J. Phys. B **28**, L77 (1995)].

[3] The derivation of this result will be published elsewhere.

[4] P. Mohr is now working on the extraction of this correction from his respective high $Z\alpha$ results [P. Mohr (private communication)].

TABLE IV. $2S_{1/2}$-$2P_{1/2}$ Lamb shift.

ΔE (kHz)
1057845(9)[a]
1057857.6(2.1)[b]
1057839(12)[c]
1057810(4)(4)[d]
1057829(4)(4)[e]
1057854(16)[f]
1057835(15)[g]
1057847(13)[h]

[a]Experimental result, Ref. [5].
[b]Experimental result, Refs. [6,7].
[c]Experimental result, Ref. [8].
[d]Theory, this work, and $r_p = 0.805(11)$ fm, Ref. [37].
[e]Theory, this work, and $r_p = 0.862(12)$ fm, Ref. [38].
[f]Self-consistent $1S$, Ref. [3].
[g]Self-consistent $1S$, Refs. [2,1].
[h]Self-consistent $1S$, Ref. [4].

Next we turn to the discussion of the $1S$ Lamb shift. Unfortunately, its extraction from the experimental data is less straightforward. The experimentalists managed to separate measurement of the $1S$ Lamb shift from the measurement of the Rydberg constant by comparing the frequencies of two transitions with different main quantum numbers and excluding the large level separation depending on the Rydberg constant. In this manner certain combinations of $1S$, $2S$, and higher level Lamb shifts are experimentally obtained. It is pretty easy to compare these experimental data in [1–4] with the theory above and after trivial calculations we find excellent agreement between the theory and experiment. We will not discuss these results here.

Unbiased extraction of the $1S$ Lamb shift from the experimental data is still a problem. It is impossible to avoid using to this end the experimental value of the $2S$ Lamb shift and the emerging value of the $1S$ Lamb shift thus depends on the experimental result for the $2S_{1/2}$-$2P_{1/2}$ splitting. Higher level Lamb shifts, which also enter the problem, may be calculated with sufficient accuracy. The standard approach accepted by all experimental groups consists in adopting one or the other $2S_{1/2}$-$2P_{1/2}$ experimental result and thus extracting the value of the $1S$ Lamb shift. All values in Table I for the $1S$ Lamb shift are obtained in this manner with the help of experimental values in [5] or in [8] for the classic Lamb shift. These values should be compared with our theoretical prediction

$$\Delta E_L(1S) = 8\,172\,729(28)(32)\ \text{kHz}, \tag{11}$$

where again the first error is determined by the yet uncalculated contributions to the Lamb shift and the second reflects the experimental uncertainty in the measurement of the proton rms charge radius.

The results of all experiments mentioned in Table I are pretty consistent and their agreement with the theoretical value in Eq. (11) is satisfactory but not spectacular. It is necessary to recollect at this point that the experimental values in the table depend on the experimental value of the $2S_{1/2}$-$2P_{1/2}$ Lamb shift adopted in their extraction and the change of the $1S$ Lamb shift value under transition from one experimental $2S_{1/2}$-$2P_{1/2}$ Lamb shift value to another may be significant.

It would be helpful to find a way to extract the value of the $1S$ Lamb shift from the experimental data unambiguously without reference to the $2S_{1/2}$-$2P_{1/2}$ experimental results, which, while being compatible with the theory, seem to be somewhat larger than the theoretical prediction. A natural way to reach this goal is to use the theoretical relation between the $1S$ and $2S$ Lamb shifts. A good deal of theoretical contributions to the Lamb shift scale as n^3 and hence vanish in the difference $8E_L(2S) - E_L(1S)$. In particular, all main sources of the theoretical uncertainty, namely, the proton charge radius contribution and almost all yet uncalculated corrections to the Lamb shift mentioned above vanish. A significant contribution to this difference may be produced only by the term of the form $\alpha^2(Z\alpha)^6 \ln^2(Z\alpha)^{-2}$, which was calculated recently [7]. This term produces correction about 14 kHz and the accuracy of the difference under consideration is determined by the yet uncalculated single logarithmic contribution of the same order. Such a term would not change the square of the logarithm term by more than 50% and hence the uncertainty of the difference under consideration is about 7 kHz. Hence we obtain the relation

$$8E_L(2S) - E_L(1S) = \Delta, \tag{12}$$

where $\Delta = 187\,234(7)$ kHz. The importance of this relation for the Lamb shift problem was emphasized in [7].

Now one may obtain self-consistent values for the $1S$ Lamb shift directly from the experimental data in Refs. [3,4,2] with the help of the relations

$$E_L(1S) = \frac{8}{3}(F_{1S-2S} - 4F_{2S-4S_{1/2}}) - \frac{32}{3}E_L(4S_{1/2}) + \frac{5}{3}\Delta, \tag{13}$$

$$E_L(1S) = \frac{8}{3}(F_{1S-2S} - 4F_{2S-4P_{1/2}}) - \frac{32}{3}E_L(4P_{1/2}) + \frac{5}{3}\Delta, \tag{14}$$

$$E_L(1S) = \frac{40}{19}(F_{1S-2S} - \frac{16}{5}F_{2S-8D_{5/2}}) - \frac{128}{19}E_L(8D_{5/2}) + \frac{21}{19}\Delta. \tag{15}$$

Numerical results are presented in Table V. These results have somewhat larger errors than the respective results in Table I; however, they do not depend on the experimental value of the $2S_{1/2}$-$2P_{1/2}$ Lamb shift and on the value of the proton charge radius. The accuracy of the self-consistent numbers in Table V is mainly determined by the accuracy of the frequency measurements in [3,2,4]. A factor 4–5 reduction of the experimental errors would lead to a self-consistent determination of the $1S$ Lamb

TABLE V. $1S$ Lamb shift.

ΔE (kHz)
8172915(129)[a]
8172763(117)[b]
8172858(107)[c]
8172729(28)(32)[d]

[a]Self-consistent value, Ref. [3].
[b]Self-consistent value, Refs. [2,1].
[c]Self-consistent value, Ref. [4].
[d]Theory, this work.

shift with the same accuracy as for the values cited in Table I. One may even invert the usual approach to the $2S_{1/2}$-$2P_{1/2}$ and $1S$ Lamb shift values and extract values of the $2S$-$2P$ Lamb shift from the respective self-consistent $1S$ values (see three last lines in Table IV). These values of the $2S_{1/2}$-$2P_{1/2}$ Lamb shift are consistent with the results of the direct measurements of the $2S_{1/2}$-$2P_{1/2}$ Lamb shift but have somewhat larger error bars. However, self-consistent values of the $2S_{1/2}$-$2P_{1/2}$ Lamb shift would become quite competitive with the results of the direct measurements after the 4–5 times reduction of the current experimental errors in the frequency measurements is achieved.

The reduction of the errors of the values of the $1S$ and $2S_{1/2}$-$2P_{1/2}$ Lamb shifts opens ways to a more precise determination of the Rydberg constant. We would like to mention two alternative directions in the determination of the Rydberg constant value besides the one adopted now (see, e.g., [1,2]). First, one can use the self-consistent value of the $1S$ Lamb shift and the respective $2S_{1/2}$-$2P_{1/2}$ Lamb shift to get the value of the Rydberg constant. Today such an approach leads to a loss of accuracy in comparison with the current experimental value of the Rydberg constant (see Table VI, where the first error in the self-consistent values of the Rydberg constant is determined by the accuracy of the self-consistent Lamb shift values, the second is determined by the accuracy of the frequency measurement, and the third is determined by the accuracy of the electron-proton mass ratio [39]), but greater accuracy may be achieved in the future. An important advantage of such an approach is that the value obtained in this way is independent of the direct experimental results on the $2S_{1/2}$-$2P_{1/2}$ Lamb shift and of the value of the proton charge radius. The second approach is simply to reject the experimental data on the Lamb shifts and to directly use for the determination of the Rydberg constant the data on the frequencies of transitions between the levels with different main quantum numbers. Such an approach becomes feasible now since the accuracy of the theoretical expression for such transitions is defined by the theoretical error of the expression for the $1S$ (or $2S$) Lamb shift, which is about 28 kHz (and even smaller for the $2S$ Lamb shift), as discussed above, and is thus smaller than the experimental error of the frequency determination. Respective values of the Rydberg constant are again presented in Table VI, where the first error is determined by the accuracy of the theoretical expression, the second is defined by the experimental error of the frequency measurement, the third is determined by the experimental error in the determination of the proton charge radius, and the fourth is determined by the accuracy of the electron-proton mass ratio. The values of the Rydberg constant in the last two lines in Table VI derived from independent experimental data [2,1] are pretty consistent. These values are slightly more accurate than the ones obtained by other methods and are among the most precise contemporary values of this constant. A natural drawback of this approach is, of course, the dependence of the obtained value of the Rydberg constant on the proton charge radius.

TABLE VI. Rydberg constant.

R_∞ (cm^{-1})
109737.3156841(42)[a]
109737.3156834(24)[b]
109737.3156868(58)(20)(12)[c]
109737.3156811(52)(14)(12)[d]
109737.3156797(12)(20)(14)(12)[e]
109737.3156802(05)(14)(06)(12)[f]

[a]Experimental value, Ref. [1].
[b]Experimental value, Ref. [2].
[c]Self-consistent value, Refs. [1,3].
[d]Self-consistent value, Refs. [2,1].
[e]Theory, this work, and Ref. [1].
[f]Theory, this work, and Ref. [2].

In conclusion, we would like to emphasize that the high accuracy of the Lamb shift theory opens perspectives in the determination of the Rydberg constant and of the Lamb shift in the $1S$ and $2S$ states. Five directions of experimental investigations, namely, more precise measurement of the transitions between levels with different main quantum numbers, more precise measurements of the $1S$ and $2S$ Lamb shifts, a more precise measurement of the electron-proton mass ratio, and a direct measurement of the proton charge radius, seem especially promising. It is very important that all these experiments are mutually complementary since they may lead to the values of the Rydberg constant of comparable accuracy based on the different kinds of experimental data. On the theoretical side, the calculation of the still unknown corrections to the energy levels discussed above, with the goal of the reduction of the theoretical error in the determination of the $1S$ Lamb shift to the level of 1 kHz (and, respectively, of the $2S$ Lamb shift to several tenths of a kHz), seems to be both necessary and feasible.

We are deeply grateful to S. G. Karshenboim, who took part in the initial stage of this project as described in [20,21]. M. E. is deeply grateful to H. Grotch for fruitful collaboration on the other corrections of order $\alpha^2(Z\alpha)^5$ to the Lamb shift and for numerous helpful discussions. We are indebted to P. Mohr for helpful communications on the vacuum polarization contributions to the Lamb shift and for providing us with his results prior to publication. We highly appreciate useful communications with M. Boshier on the preliminary results of the measurement of the $1S$ Lamb shift [4]. M. E. acknowledges

helpful discussions on the physics of hyperfine splitting and the Lamb shift with T. Kinoshita, D. Owen, and K. Pachucki. The analytic calculations above were partially performed with the help of the REDUCE symbolic computation software. Final numerical calculations with the help of the VEGAS computer program were conducted at the Maui High Performance Computing Center and we highly appreciate the opportunity to use these facilities. Through the use of the MHPCC, this research was sponsored in part by the Phillips Laboratory, Air Force Materiel Command, USAF, under Contract No. F29601-93-2-0001. Part of this work was done during the visit of M.E. to Pennsylvania State University. He is deeply grateful to his colleagues at the Physics Department of Pennsylvania State University and especially to H. Grotch for kind hospitality. The research described in this publication was made possible in part by Grant No. RZE300 from the International Science Foundation and was also supported by the Russian Foundation for Fundamental Research under Grant No. 93-02-3853. The work of M.E. was supported in part by the National Science Foundation under Grant No. NSF-PHY-9120102.

---

* Electronic-mail address: eides@lnpi.spb.su

[1] T. Andreae *et al.*, Phys. Rev. Lett. **69**, 1923 (1992).
[2] F. Nez *et al.*, Europhys. Lett. **24**, 635 (1993).
[3] M. Weitz *et al.*, Phys. Rev. Lett. **72**, 328 (1994).
[4] D. Berkeland, M. Boshier, and E. Hinds (unpublished).
[5] S. R. Lundeen and F. M. Pipkin, Phys. Rev. Lett. **46**, 232 (1981); Metrologia **22**, 9 (1986).
[6] Yu. L. Sokolov and V. P. Yakovlev, Zh. Eksp. Teor. Fiz. **83**, 15 (1982) [Sov. Phys. JETP **56**, 7 (1982)]; V. G. Palchikov, Yu. L. Sokolov, and V. P. Yakovlev, Pis'ma Zh. Eksp. Teor. Fiz. **38**, 347 (1983) [JETP Lett. **xx**, xxx (19xx)].
[7] S. G. Karshenboim, Zh. Eksp. Teor. Fiz. **106**, 1105 (1994) [JETP **79**, 230 (1994)].
[8] E. W. Hagley and F. M. Pipkin, Phys. Rev. Lett. **72**, 1172 (1994).
[9] F. G. Mariam *et al.*, Phys. Rev. Lett. **49**, 993 (1982).
[10] V. W. Hughes, Nucl. Phys. A **463**, 3c (1987).
[11] M. I. Eides, S. G. Karshenboim, and V. A. Shelyuto, Phys. Lett. B **229**, 285 (1989); Yad. Fiz. **50**, 1636 (1989) [Sov. J. Nucl. Phys. **50**, 1015 (1989)].
[12] M. I. Eides, H. Grotch, and D. A. Owen, Phys. Lett. B **294**, 115 (1992).
[13] M. I. Eides, S. G. Karshenboim, and V. A. Shelyuto, Phys. Lett. B **249**, 519 (1990).
[14] M. I. Eides, S. G. Karshenboim, and V. A. Shelyuto, Phys. Lett. B **268**, 433 (1991); **316**, 631(E) (1993); **319**, 545(E) (1993); Yad. Fiz. **55**, 466 (1992); [Sov. J. Nucl. Phys., **55** 257 (1992)]; **57**, 1343(E) (1994) [xx, xxxx (19xx)].
[15] T. Kinoshita and M. Nio, Phys. Rev. Lett. **72**, 3803 (1994).
[16] M. I. Eides and H. Grotch, Phys. Lett. B **301**, 127 (1993).
[17] M. I. Eides and H. Grotch, Phys. Lett. B **308**, 389 (1993).
[18] M. I. Eides, H. Grotch, and P. Pebler, Phys. Lett. B **326**, 197 (1994); Phys. Rev. A **50**, 144 (1994).
[19] K. Pachucki, Phys. Rev. A **48**, 2609 (1993).
[20] M. I. Eides, S. G. Karshenboim, and V. A. Shelyuto, Phys. Lett. B **312**, 358 (1993); Yad. Fiz. **57**, 1309 (1994) [Phys. At. Nucl. **57**, xxx (1994)].
[21] M. I. Eides, S. G. Karshenboim, and V. A. Shelyuto, Yad. Fiz. **57**, 2246 (1994) [Phys. At. Nucl. **57**, xxx (1994)].
[22] K. Pachucki, Phys. Rev. Lett. **72**, 3154 (1994).
[23] M. I. Eides, S. G. Karshenboim, and V. A. Shelyuto, Ann. Phys. (N.Y.) **205**, 231 (1991).
[24] H. M. Fried and D. R. Yennie, Phys. Rev. **112**, 1391 (1958).
[25] M. I. Eides, Pennsylvania State University Report No. PSU/TH/149, 1994 (unpublished); *Proceedings of the Paris Workshop on Quantum Infrared Physics*, edited by H. Fried (World Scientific, Singapore, in press).
[26] M. E. Cage *et al.*, IEEE Trans. Instrum. Meas. **38**, 284 (1989).
[27] T. Appelquist and S. J. Brodsky, Phys. Rev. Lett. **24**, 562 (1970); Phys. Rev. A **2**, 2293 (1970).
[28] R. Barbieri, J. A. Mignaco, and E. Remiddi, Nuovo Cimento A **6**, 21 (1971).
[29] R. Karplus, A. Klein, and J. Schwinger, Phys. Rev. **86**, 288 (1952).
[30] M. Baranger, H. A. Bethe, and R. P. Feynman, Phys. Rev. **92**, 482 (1953).
[31] J. Sapirstein and D. R. Yennie, in *Quantum Electrodynamics*, edited by T. Kinoshita (World Scientific, Singapore, 1990), p. 560
[32] H. Grotch, in *Proceedings of the Paris Workshop on Quantum Infrared Physics* (Ref. [25]).
[33] K. Pachucki, Ann. Phys. (N.Y.) **226**, 1 (1993).
[34] S. G. Karshenboim, Zh. Eksp. Teor. Fiz. **103**, 1105 (1993) [JETP **76**, 541 (1993)].
[35] P. Mohr (unpublished).
[36] A. van Wijngaarden, J. Kwela, and G.W.F. Drake, Phys. Rev. A **43** 3325 (1991).
[37] D. J. Drickey and L. N. Hand, Phys. Rev. Lett. **9**, 521 (1962); L. N. Hand, D. J. Miller, and R. Wilson, Rev. Mod. Phys. **35**, 335 (1963).
[38] G. G. Simon, Ch. Schmidt, F. Borkowski, and V. H. Walther, Nucl. Phys. A **333**, 381 (1980).
[39] Particle Data Group, Phys. Rev. D **50**, 1173 (1994).
[40] K. Pachucki and H. Grotch, Phys. Rev. A **51**, 1854 (1995).
[41] M. Eides and H. Grotch, Pennsylvania State University Report No. PSU/TH/151/ hep-ph/9411220 (unpublished), Phys. Rev. A (to be published).
[42] E.A. Golosov, I.B. Khriplovich, A.I. Milstein, and A.S. Yelkhovsky, Budker Institute of Nuclear Physics Report No. BINP 94-79, 1994 (unpublished); Zh. Eksp. Teor. Fiz. **107**, 393 (1995).